

Lateral migration of vesicles in microchannels: effects of walls and shear gradient

Migration latérale de vésicules dans des microcanaux : effets des parois et du gradient de cisaillement

BADR KAOUI, GWENNOU COUPIER¹, CHAOUQI MISBAH, THOMAS PODGORSKI,

Laboratoire de Spectrométrie Physique, CNRS - UMR 5588,

Université Grenoble I, B.P. 87, 38402 St Martin d'Hères Cedex, France

bkaoui@spectro.ujf-grenoble.fr, gcoupier@spectro.ujf-grenoble.fr, cmisbah@spectro.ujf-grenoble.fr, tpodgors@spectro.ujf-grenoble.fr

Cross-streamline migration of a vesicle in a bounded Poiseuille flow is investigated experimentally and numerically. The combined effects of the shear gradient of the flow and of walls induce a migration of the vesicle towards the center-line of the channel. A migration law (as a function of relevant structural and flow parameters) is presented. This similarity law is compared with the laws governing the migration velocity of a vesicle in an unbounded Poiseuille flow and in a shear flow near a wall. The relative contributions of both effects are discussed.

Nous étudions la migration transverse d'une vésicule dans un écoulement de Poiseuille confiné à l'aide d'expériences et de simulations. La vésicule migre vers le centre de l'écoulement sous l'effet combiné du gradient de cisaillement et de la présence de parois. Nous présentons une loi de migration donnant la vitesse de migration en fonction des différents paramètres caractérisant la vésicule et l'écoulement. Cette loi est comparée avec les lois donnant la vitesse de migration d'une vésicule dans un écoulement de Poiseuille non borné ainsi que dans un écoulement de cisaillement borné par une paroi. Le poids relatif de chacun de ces contributions est discuté.

I ■ INTRODUCTION

Vesicles are closed phospholipid membranes ; they encapsulate an internal fluid and are usually suspended in an external aqueous solution. Physics of vesicles has attracted much interest in the recent decades and has been the subject of many theoretical and experimental works [1]. This is because of their ability to reproduce some dynamical behaviours observed for living cells (such as red blood cells) and the interest to exploit them as carriers of biomaterials (for example drugs). Understanding the dynamical behavior of such deformable entities (orientation, deformation and migration) when its suspending fluid is subject to shear, is a fundamental question and a crucial key to design microfluidic devices with abilities to sort out and separate entities basing on their mechanical properties (size, deformability, encapsulated fluid...etc.) [2]. Likewise, lateral migrations induce non uniform lateral distributions of the suspended entities, which have important consequences on the rheology of a confined suspension (e.g. the Fahraeus-Lindquist effect in blood vessels [3]).

In the present work we investigate how Poiseuille flow in a microchannel induces lateral migration of a single vesicle. The Stokes limit (very small Reynolds numbers values) is considered, so that inertia can be neglected and therefore no inertial lift force would be expected. Vesicles dynamics under an external applied simple shear flow has been the subject of extensive studies, both in unbounded geometries [4-8] as well as in the presence of a bounding wall [9-13]. A vesicle placed in an unbounded fluid subject to simple shear (in the Stokes limit) does not exhibit any lateral migration with respect to the flow direction. When the viscosity ratio between the inner and the outer fluids is small, it performs a tank-treading dynamics where the orientation of the main axis of the vesicle is constant and the membrane undergoes a tank-treading motion. If the suspended fluid is bounded by a wall, which breaks the translational symmetry perpendicular to the flow direction as well as the upstream-downstream symmetry, a tank-treading vesicle migrates away from the wall. This viscous lift force is caused by the flow induced fore-aft symmetry breaking of the vesicle's shape [10]. Recently, we also found that even in unbounded geometry, the non linear character of the Poiseuille flow velocity profile (non uniform shear rate) induces lateral migration of vesicles towards the

1. Corresponding author

flow center-line [14]. For a vesicle suspended in a fluid flowing in a microchannel (the case considered here), the two situations mentioned above coexist simultaneously. The microchannel wall and the Poiseuille flow both participate to push the vesicle toward the center-line of the channel, where a steady axisymmetric stage is reached. This final stage has been described in several papers [15-17]. Migration has also been reported on capsules [18-20] red blood cells [19,20] and drops [21,22].

Experiments as well as simulations are carried out in order to study the interplay between these two effects. In [23], we presented a law for the vesicle lateral migration in a microchannel, which depends on the geometry of the channel, on the Poiseuille flow parameters and on the intrinsic properties of the vesicle. In the following, we describe the experimental and numerical methods with more details. Thanks to complementary simulations, we are also able to discuss the relative importance of the wall and of the non uniformity of the shear rate in pushing a vesicle towards the centerline.

II ■ GENERAL FRAMEWORK

The microfluidic channel is straight and has a rectangular cross section. The flow direction is Ox , and the lateral migration is along Oy ; this means that migration is studied for a given position Z . Let $2w$ denote the channel width in the y direction, and v_0 the imposed flow velocity at the center of the channel in the absence of vesicle. The two walls are located at $y = 0$ and $y = 2w$. A vesicle, whose membrane is incompressible, is characterized by two geometrical parameters: its effective radius R , determined from its incompressible volume V by $R_0 = (3V/4\pi)^{1/3}$ and its reduced volume $\nu = V/\left[4\pi(S/4\pi)^{3/2}/3\right]$ (S is the area of the vesicle) characterizing vesicle deflation. The reduced volume is the vesicle volume divided by the volume of a sphere of same area: it is thus lower or equal to 1. Volumes are calculated by assuming axisymmetric shapes along the vesicle's main axis. The viscosity ratio is defined as $\lambda = \eta_{in}/\eta_{out}$, where η_{in} and η_{out} denote the inner and the outer viscosity, respectively. A summary of the explored parameters ranges is presented in *Tab. 1*. Note that explored parameters in the plane (λ, ν) are such that the dynamics is of tank-treading type [4-8].

The dynamics depends a priori on five key parameters $(R_0, w, v_0, \nu, \lambda)$. Our strategy is to consider first the case

with no viscosity contrast ($\lambda \approx 1$) while the reduced volumes fall within a fixed narrow range. The three other key parameters are then varied in order to find a migration law. We also show that this law is valid for other values of λ and ν . This law is compared to the laws found in the unbounded case and for a vesicle in a simple shear flow near wall.

III ■ METHODS

● III.1 EXPERIMENTAL METHOD

The microfluidic device is composed of straight channels of height $h_0 = 66\mu\text{m}$ (in the direction of gravity z) and width $2w$ (rectangular cross section). The walls of the channels are made of PDMS glued to a glass cover slide. The flow is induced by applying a pressure difference between the inlet and the outlet which are linked to reservoirs placed at different heights. Vesicles are prepared following the electroformation method [24]. They are made of a DOPC lipid bilayer enclosing an inner solution of sugar (sucrose or glucose) in water or in a 1 : 4 glycerol-water ($w : w$) mixture. Samples are diluted in a slightly hyperosmotic outer solution of the same type, in order to deflate them by osmosis. Dextran can be added to one of the solutions to modify the viscosity ratio λ .

A particular design of the upstream channel creates an initial condition where incoming vesicles touch the $y = 0$ wall in the observation area and start to be lifted away from it (see *Fig. 1*). In particular, they have already developed a nearly ellipsoidal shape tilted with respect to the wall [10-12]. Moreover, the flow has been established for a long time, resulting in centering in the z direction. In that case, the 2D fluid velocity profile in the xy plane where the vesicle lies is nearly parabolic, provided the rectangular cross section of the 3D channel obeys $2w/h_0 \leq 3$ [25]. Therefore, as a first approximation, the vesicle is in a 2D Poiseuille flow, with reproducible initial conditions $y(t=0) = y_0$, where y_0 is the position of the center of mass just before lift-off, which is close to R_0 . As the vesicle is centered in the Z -direction, the imposed profile is thus written as $v_x^\infty(\vec{r}) = c(yw - y^2/2)$, where $c = 2v_0/w^2$ is the curvature of the parabolic velocity profile. The vesicle is tracked along its trajectory with a phase contrast microscope, and the position y of its center of mass is determined by image processing.

Table 1 : Summary of the parameters ranges explored in this work. The solutions are of density and viscosity close that of water; therefore the Reynolds number are lower than 10^{-2} .

	R_0 (μm)	w/R_0	v_0 ($\mu\text{m} \cdot \text{s}^{-1}$)	ν	λ
Experiments	$9.3 \leq R_0 \leq 23.1$	$1.9 \leq w/R_0 \leq 8.8$	$30 \leq v_0 \leq 1400$	$0.82 \leq \nu \leq 0.99$	$\lambda = 1.1, 5.8, 10$
Simulations	$R_0 = 10$	$8 \leq w/R_0 \leq 14$	$500 \leq v_0 \leq 800$	$0.89 \leq \nu \leq 0.99$	$\lambda = 1$

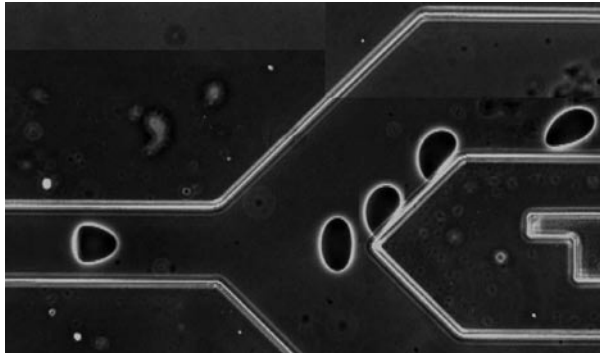


Figure 1 : Phase contrast microscopy image of the Y-junction allowing to get reproducible initial conditions to study the lift force (the flow is from left to right): the initially centered vesicle follows the central streamline and is pushed against the wall at the bifurcation. Then it enters one of the two branches, which are equivalent, from which point its trajectory is studied. The channel's width is 135 microns on the right.

● III.2 SIMULATION METHOD

III.2.1 Hydrodynamical equations

In the simulations, two-dimensional neutrally buoyant vesicles are considered (the same mass density ρ inside and outside the vesicle), having no viscosity contrast ($\lambda = 1$). Since the Reynolds number is low (of the order of 10^{-2}), the fluid flow inside and outside the vesicle is described by the Stokes equations :

$$-\bar{\nabla} p(\vec{r}) + \eta \bar{\nabla}^2 \vec{v}(\vec{r}) = -\delta(\vec{r} - \vec{r}_m) \vec{f}(\vec{r}), \quad (1a)$$

$$\bar{\nabla} \cdot \vec{v}(\vec{r}) = 0, \quad (1b)$$

where p is the pressure, \vec{v} is the velocity and \vec{f} the membrane force at the point \vec{r}_m , given by :

$$\vec{f} = \left[\kappa \left(\frac{\partial^2 H}{\partial s^2} + \frac{H^3}{2} \right) - H \zeta \right] \vec{n} + \frac{\partial \zeta}{\partial s} \vec{t}, \quad (2)$$

where \vec{n} and \vec{t} are the normal and the tangential unit vectors, respectively. κ is the membrane rigidity, H is the local membrane curvature and ζ a local Lagrangian multiplier introduced in order to fulfill the perimeter conservation constraint of the vesicle. Details of the derivation of the membrane force given by Eq. (2) are reported in Ref. [14]. This force has no zero value just on the membrane of the vesicle, hence the Dirac delta function in the right hand side of Eq. (1a). The membrane exerts the force given by Eq. (2) on its surrounding fluid as a response to the external hydrodynamical stresses that tend to bend it.

III.2.2 Boundary conditions

The above Stokes equations (1) are solved for the following boundary conditions : 1 - the velocity continuity across the membrane, because of the non-slip boundary condition and of the impermeability of the vesicle membrane, 2 - the hydrodynamical stress jump across the membrane is equal to the membrane force and 3 - the velocity of the external suspending fluid is undisturbed at distances far from the location of the vesicle membrane.

III.2.3 Boundary integral method

Thanks to the linearity of Eqs. (1), they are solved using the boundary integral method, which is a technique based on the Green's functions [26]. Its adaptation to vesicle problems can be found in Refs [5,11,14,27]. The membrane velocity is given by the following integral equations, which are solved numerically :

$$v_i(\vec{r}_m) = \frac{1}{4\pi\eta} \oint G_{ij}^w(\vec{r}_m, \vec{r}') f_j(\vec{r}') ds(\vec{r}') + v_i^\infty(\vec{r}_m), \quad (3)$$

where G_{ij}^w is the Green's function for the fluid bounded by a steady infinite plane wall located at $y = 0$:

$$G_{ij}^w(\vec{r}, \vec{r}') = G_{ij}(\vec{r} - \vec{r}') - G_{ij}(\vec{r} - \vec{r}'_l) + 2r'_y G_{ij}^D(\vec{r} - \vec{r}') - 2r'_y G_{ij}^{SD}(\vec{r} - \vec{r}'_l). \quad (4)$$

$G_{ij}(\vec{r}) = -\delta_{ij} \ln r + \frac{r'_i r'_j}{r^2}$ is the Green's function for an unbounded fluid, called also Stokeslet, $\vec{r}'_l = (r'_x, -r'_y)$ is the image of \vec{r}' with respect to the wall. The function

$$G_{ij}^D(\vec{r}) = (\delta_{jx} - \delta_{jy}) \left(\frac{\delta_{ij}}{r^2} - 2 \frac{r'_i r'_j}{r^2} \right) \quad (5)$$

is the Stokeslet doublet, and

$$G_{ij}^{SD}(\vec{r}) = r'_y G_{ij}^D(\vec{r}) + (\delta_{jx} - \delta_{jy}) \frac{\delta_{jy} r'_i - \delta_{iy} r'_j}{r^2} \quad (6)$$

is the source doublet. $r \equiv |\vec{r}|$ and r_i is the i^{th} component of the vector \vec{r} . The evolution of the vesicle shape and its location is obtained by updating every membrane node using a Euler scheme : $\vec{r}_m(t + \Delta t) = \vec{v}(\vec{r}_m, t) \Delta t + \vec{r}_m(t)$.

IV ■ RESULTS FOR $\lambda \approx 1$

● IV.1 EXPERIMENTAL RESULTS

The experimental evolution with time of the lateral position y of the center of mass of a vesicle with $\lambda = 1.1$ is

shown in Fig. 2a. The vesicle quickly moves away from the wall, then the migration velocity decreases to zero as it approaches the center-line. Along this trajectory, it continuously deforms from a tilted ellipsoid to an axisymmetric bullet-like shape. For a given reduced volume, the function $y(t)$ depends a priori on the three parameters (R_0 , w , v_0).

In order to determine the functional dependence of the migration velocity, space and time variables are rescaled. In both simple shear flow cases and unbounded Poiseuille, the only space scale is given by vesicle's size R_0 . Coherently, the dimensionless position $\hat{y} = y/R_0$ is introduced. The reduced half-width of the channel will be noted $\hat{w} = w/R_0$. However, the choice of a relevant time (or velocity) scale is less obvious. Indeed, while the inverse of the shear rate yields a natural scale, this cannot be an adequate choice since the shear rate is not constant along the trajectory. The trick is to rescale each infinitesimal time t step around the time by the local shear rate $\dot{\gamma}(y) = dv_x^x/dy = c(w-y)$ of the unperturbed flow at the position $y(t)$. Note that it amounts to saying that the migration velocity is controlled by the local flow, which is a reasonable assumption in a Stokes flow. Nonetheless, working directly with the velocity $\dot{y}(y)$ instead of the position $y(t)$ is less easy when starting with experimental data, because of the noise due to discrete time derivation of the position, which is known with a limited precision. Then the choice was made to work directly on the raw data y and t . The new dimensionless time-like parameter is obtained by integrating the rescaled time steps :

$$\hat{t} = \int_0^t \dot{\gamma}(y) d\tau = c \int_0^t [w - y(\tau)] d\tau \quad (7)$$

\hat{t} accounts for the history of the shear rates experienced by the vesicle along its trajectory. The raw data for the migration velocity spread over more than a decade in the parameters space. Interestingly, as shown in Fig. 2b, all experimental curves $\hat{y}(\hat{t})$ collapse, whatever the values of R_0 , w , and v_0 within the explored range $0.95 \leq v \leq 0.97$. A log-log plot of this master $\hat{y}(\hat{t}) - \hat{y}_0$ curve is linear, a clear signature of a power law behavior $\hat{y}(\hat{t}) - \hat{y}_0 = \beta \hat{t}^\alpha$, where the dimensionless parameters α and β , that are independent from R_0 , w and v_0 , are obtained from the data fit. Such collapse was found for all other studied reduced volumes [23]. By taking the $1/\alpha$ power of the latter relation before derivating, the lateral migration velocity as $v_m = \dot{y}$ a function of the position y and the triplet (R_0 , W , v_0) is then easily extracted :

$$v_m = \xi c R_0^2 \frac{\hat{w} - \hat{y}}{(\hat{y} - \hat{y}_0)^\delta} = \xi \frac{R_0 \dot{\gamma}(y)}{(\hat{y} - \hat{y}_0)^\delta} \quad (8)$$

This similarity law is the main results of our work and the basis for the discussions to come. In the range $0.95 \leq v \leq 0.97$, one finds $\xi \equiv \alpha \beta^{1/\alpha} = 1.3 \times 10^{-2} \pm 0.3 \times 10^{-2}$ and $\delta \equiv 1/\alpha - 1 = 0.8 \pm 0.2$. The error bars for these coefficients can be linked with the error bars on y and w due to local defects on the PDMS walls, and also (and mainly) with the uncertainties on the measure of v , which requires a very precise determination of the membrane position. Since, as we shall see, the velocity depends on the reduced volume, this can lead to uncertainties on the determination of the coefficients.

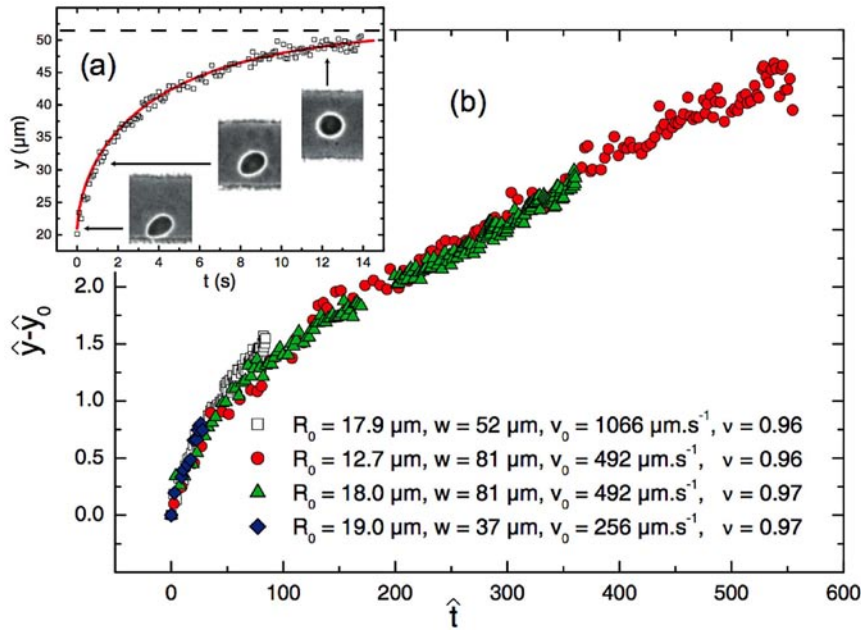


Figure 2 : (a) : Experimental time evolution of the lateral position y for a vesicle with $\lambda = 1.1$ (scatter). The dashed line indicates the center-line. The solid line shows the $y(t)$ curve obtained from the numerical resolution of Eq. (8).

(b) : Evolution of $\hat{y} - \hat{y}_0$ versus \hat{t} for four such vesicles.

Note that the differential equation (8) has no analytical solution but can be easily solved numerically. Then a fitting procedure of the experimental curve $y(t)$ can directly yield the parameters ξ and δ without going through a noise-generating rescaling of the experimental data (see Fig. 2a). This rescaling procedure was only used to find the form of the migration law since there exists no theoretical prediction we could be inspired by.

● IV.2 SIMULATION RESULTS

Vesicles with $R_0 = 10 \mu\text{m}$ and a reduced volume $\nu = 0.95$ are initially placed in five different lateral positions, one of them being intentionally placed at the flow center-line ($\hat{y} = 10$). The external applied Poiseuille flow is characterized by $v_0 = 600 \mu\text{m} \cdot \text{s}^{-1}$ and $\hat{w} = 10$. Two cases are considered here for comparison purposes. The suspending fluid is unbounded or bounded by a infinite plane wall located at $y = 0$.

For the unbounded case (Fig. 3a). All vesicles migrate laterally to the flow center-line as was reported in Ref. [14]. The center-line is their equilibrium lateral position where they move parallel to the flow direction with an axisymmetric shape (the blue colored shape in Fig. 3a). The final equilibrium lateral position location does not depend on the initial position of the vesicle.

Moreover, the problem is symmetric with respect to the location of the flow center-line, vesicle placed above or below this axis move and deform in the same fashion (see the curves and their corresponding shapes in Fig. 3a).

By placing a steady infinite plane wall at the position $y = 0$ (where the Poiseuille flow velocity vanishes), the evolution in time of the vesicle lateral position is affected (see Fig. 3b). In this case, the dynamics of the vesicle depends on the initial lateral position.

Vesicles initially placed below the center-line ($0 < y(t=0) < w$) migrate laterally until reaching an equilibrium lateral position (with a slight shift above the cen-

ter-line, which becomes negligible for $w/R_0 \geq 8$). Here the vesicle reaches this position faster compared to the unbounded case (see for example the vesicle presented with the red line in the two Figs. 3a and 3b), due to the presence of an additional lift force, linked to the presence of the wall. Even without the presence of a second (opposite) wall, the vesicle moves parallel to the flow direction with a nearly axisymmetric shape (the blue colored shape in Fig. 3b). This seems to indicate that migration forces due to the curvature dominate over wall effects near the center-line, or that the lift force due to the walls vanishes due to the local zero shear rate (in a wall-bounded shear flow, lift velocity is proportional to shear rate [13]).

In this configuration, one can compare the migration velocity with the law proposed in Eq. (8). The variations of this migration velocity v_m with \hat{y} are shown in Fig. 4 for different values of \hat{w} and v_0 . They confirm the experimental results since they are well described by the law given by Eq. (8) with $\delta \approx 0.8$ and $\xi \approx 0.1$. The agreement between experiments and simulations regarding the exponent δ is quite satisfactory. However, numerical studies overestimate the amplitude ξ . This is attributed to the 2D character (actually a translationally invariant form in the Z direction), causing an enhancement of the lift force.

Numerically, the relative importance of the wall- and curvature- induced lift forces can be captured in the non-bounded side of the suspending fluid, that is, in the $y > w$ domain : vesicles initially placed above the center-line ($w < y(t=0) < 2w$) move with negative inclination angles (the magenta and the cyan colored shapes in figure 3b) because of the shape of the Poiseuille velocity profile in this region. The vesicle presented by the cyan colored line moves very slowly towards the centerline while the one presented with the magenta colored line travels outward the center-line. It is noteworthy that in this region the two lift forces are in competition and have opposite signs : the curvature induced lift force tries to attract the vesicle toward the centerline, while the wall induced lift force even at such distance still pushes the vesicle far from the wall. Howe-

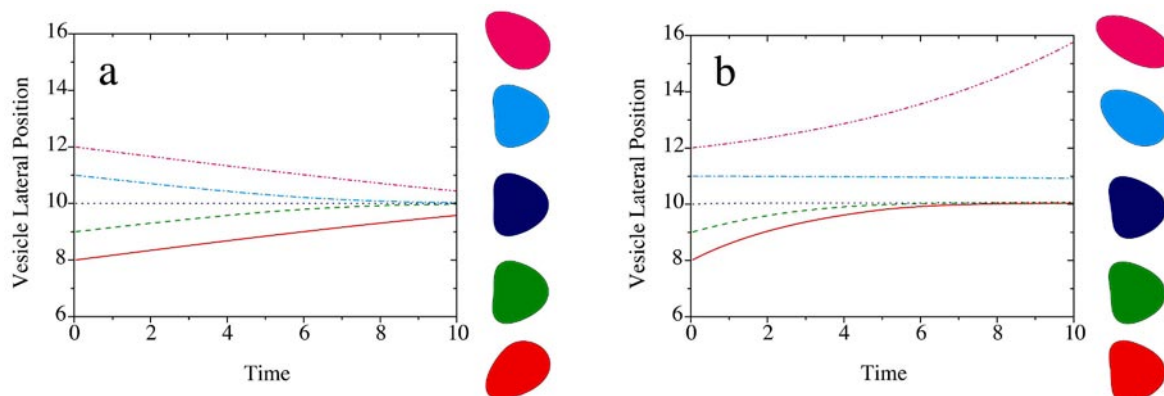


Figure 3 : Evolution in time of the vesicle lateral position in Poiseuille flow for five different initial lateral positions. (a) in unbounded fluid, (b) in a semi-infinite fluid bounded by a plane wall located at $y = 0$. In the two cases, the $v_0 = 600 \mu\text{m} \cdot \text{s}^{-1}$ and $\hat{w} = 10$ and the vesicle has a reduced volume $\nu = 0.95$. The Poiseuille flow centerline is located at $\hat{y} = 10$. Vesicle shapes shown on the right side of each plot correspond to the ones taken at time 10 and to the curve with the same color.

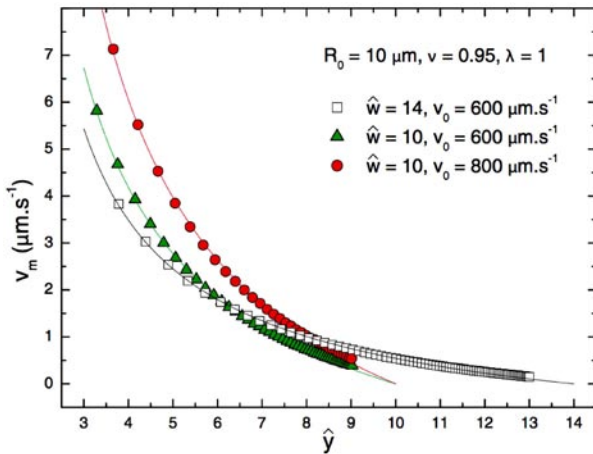


Figure 4 : Lateral migration velocity v_m of a vesicle versus its lateral position y for different W and v_0 . Scatter : simulation data; solid lines : fits with Eq. (8).

ver, their relative amplitude depends on the distance of the vesicle to the center-line. Close to the center-line, the shear rate tends to vanish and the wall induced lift force becomes weaker; this explains the inward migration of the cyan colored vesicle. Far from the center-line, the shear rates become greater which explains the outward migration of the magenta colored vesicle. Moreover, when this vesicle travels away its shape undergoes larger deformations because it finds itself in regions with higher shear rates. Note that the shear rate in that region $y > w$ has an opposite sign compared to the $y < w$ domain, but the vesicle's shape is the mirror image of the shape in the latter domain, leading to an upward lift force.

Back to the realistic case where the vesicle is placed between the wall and the center-line, we can clearly see that the effects of the walls and of the curvature of the velocity field are coupled in a non linear manner : curvature not only induces migration but also affects the shape and orientation (while in a simple shear flow they are quasi constant, whatever $\dot{\gamma}$), which affects the lift force. Indeed, the law $v_m \propto \dot{\gamma}(y)/y^\delta$ markedly differs from what was known in the previously studied cases : in an unbounded Poiseuille flow, it was shown that the migration velocity is constant but near the centre-line (where it drops to zero), as it can be seen on Fig. 3(a)[14]. On the other hand, in a simple shear flow bounded by a wall, it was theoretically [9] and experimentally [13] shown that the migration velocity is proportional to $\dot{\gamma}/y^2$. A naïve extrapolation of this result would give a velocity proportional to $\dot{\gamma}(y)/y^2$, to which a constant should be added for the curvature contribution. The result we found is far from this extrapolation, which indicates that the non-linear coupling through the shape modifications is strong. Dissipation on the walls located at $z = 0$ and $z = h_0$, which are not present in Refs. [9,13], could also modify the exponent. Further experiments with different channel depths are planned.

V ■ VARIATIONS WITH THE REDUCED VOLUME AND THE VISCOSITY RATIO

For all the values of v and λ explored here, the experimental and numerical curves $y(t)$ are still very well fitted by the theoretical law given by the resolution of Eq. (8). For the sake of comparison, it is then convenient to rescale the migration velocity in such a way that it does not depend either on R_0 , nor on w and v_0 :

$$\hat{v}_m \equiv v_m / [R_0 \dot{\gamma}(y)] = \xi / (\hat{y} - \hat{y}_0)^\delta. \quad (9)$$

Values for \hat{v}_m at $\hat{y} = 4$ are reported on Fig. 5. As discussed in Ref. [23], deflating not too viscous vesicles increases their ability to migrate. However, for high enough λ , deflating too much a vesicle can lead to a slow down in the migration (which remains directed towards the center-line). This non-monotonous behavior of the velocity was found by Olla in the case of vesicles placed in a simple shear flow bounded by a wall [9]. It can be understood with simple geometry arguments. A spherical vesicle ($v = 1$) should not migrate owing to the fore-aft symmetry. As soon as it is not spherical, the vesicle has an elongated shape, whose direction is in first approximation given by the direction of the elongational component of the flow, which is 45° relatively to the flow direction. The rotational part of the flow makes the vesicle's membrane and the inner fluid rotate. The more deflated (thus elongated) the vesicle, the more important the induced dissipation inside the vesicle. Consequently, vesicles tend to align with the flow direction in order to minimize this dissipation, resulting in an equilibrium angle between 0 and 45 degrees, which decreases when v decreases and when λ increases [4-9], as can be clearly seen on Fig. 6. In the 0 angle configuration, another fore-aft symmetry is reached, and no migration should occur. From these considerations one can infer a maximal velocity at a given value of v . Beyond the 0 angle configuration, the vesicle switches to tumbling motion. Note that when $\lambda \approx 1$, the 0 angle configuration is never reached,

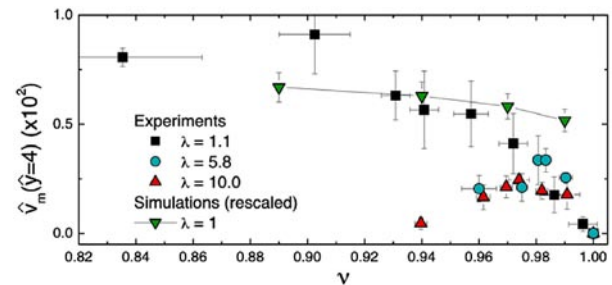


Figure 5 : Reduced migration velocity \hat{v}_m of a vesicle at position $\hat{y} = 4$ versus its reduced volume. Experimental values are calculated using Eq. (8) with the adjusted ξ and δ . For readability, the simulations data are uniformly rescaled by a factor ≈ 0.1 . Values for $\lambda \neq 1$ are not available through the simulations.

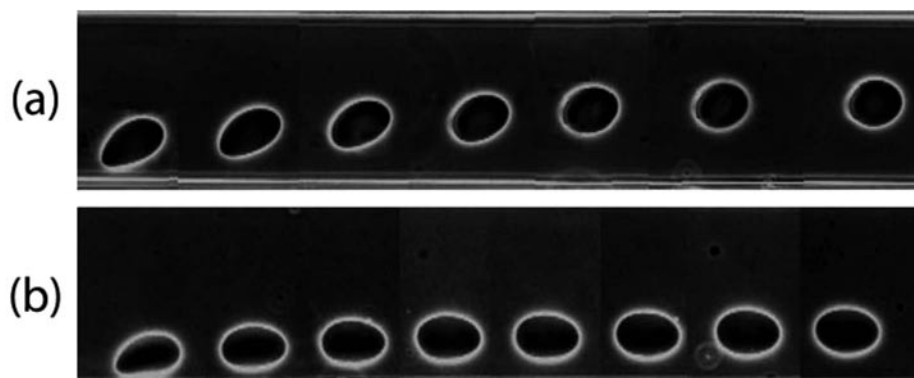


Figure 6 : Migration of two vesicles of similar size and deflation and in the same flow. (a) $\lambda = 1.1$. (b) $\lambda = 10.0$. The more viscous vesicle has a smaller angle relatively to the flow, and eventually gets a shape which is quasi symmetric between the front and the rear.

while for $\lambda \approx 6$ it is reached for $v \approx 0.93$ according to the Keller and Skalak model [4]. Coherently, no maximum is found for $\lambda \approx 1$ by Olla, while for $\lambda \approx 6$ it is found at $v = 0.98$. In our case, two effects could move these locations. First, the 0 angle position and transition to tumbling would be probably found for lower values of v in the presence of walls, which prevent any tumbling motion that would require to “push” water around the vesicle [28]. Secondly, migration towards the center-line favors the recovering of a fore-aft symmetry, since in the center the main axis of the vesicle will be parallel to the flow. Contrary to the first one, this phenomenon could switch the maximum towards higher values for v . Finally, we observe a maximum position in the velocity around $v = 0.98$ for $\lambda \geq 5$, while no maximum is observed for $\lambda \approx 1$ within the explored range v , which are results similar to the one predicted by Olla in the simple shear flow case.

VI ■ CONCLUSION

We presented a similarity law for the lateral migration velocity of a vesicle in a bounded Poiseuille flow as a function of its distance to the walls and to the center-line, its effective radius, the channel’s width and the flow velocity. This law is still valid for a large set of reduced volumes and viscosity contrasts. Deflating a spherical vesicle increases its deformability, thus its asymmetry under shear, and leads to higher migration velocities. However, beyond a given viscosity ratio, the tank-treading to tumbling transition is approached when the deflation increases, and the migration velocity undergoes a decline which can be understood on the ground of general symmetry considerations.

Far from the center-line, the migration is mainly governed by the wall-induced lift force, while curvature-driven dominate in its vicinity. However, both effects always coexist and couple in a non linear way, giving raise to a migration law which could not be directly inferred from already known laws of more simple cases.

This work is to be completed by experiments with red blood cells, which are more deflated objects with a high viscosity contrast. When isolated, red blood cells tumble and thus no migration should occur. In the meantime, depletion zones are generally observed near the capillary walls when a red blood cells suspension flows. One can suggest several reasons for this : loss of fore-aft symmetry even in the tumbling regime due to the deformability of the red blood cell or the capillary walls, or an increase of the effective viscosity of the outer solution due to the presence of numerous other red blood cells.

VII ■ ACKNOWLEDGEMENTS

Authors thank G. Danker and V. Vitkova for fruitful discussions, P. Ballet for technical assistance, and CNES and ANR (MOSICOB) for financial support. Financial support from PAI Volubilis (grant MA/06/144) is acknowledged. G.C. acknowledges a fellowship from CNES. B.K. acknowledges PhD financial support from CNRS (grant b4/015).

VIII ■ REFERENCES AND CITATIONS

- [1] LUISI P. L., WALDE P., EDITORS (2000) — *Giant Vesicles (Perspectives in Supramolecular Chemistry)* Wiley.
- [2] PAMME N. (2007) — Continuous flow separations in microfluidic devices. *Lab on a chip*. **7** 1644
- [3] FUNG Y. C. (1993) — *Biomechanics; mechanical properties of living tissues* Springer, Berlin.
- [4] KELLER J. R., SKALAK R. (1982) — Motion of a tank-treading ellipsoidal particle in a shear flow. *J. Fluid Mech.* **120** 27
- [5] BEAUCOURT J., RIOUAL F., SÉON T., BIBEN T., MISBAH C. (2004) — Steady to unsteady dynamics of a vesicle in a flow. *Phys. Rev. E.* **69** 011906
- [6] MADER M.-A., VITKOVA V., ABKARIAN M., VIALLAT A., PODGORSKI T. (2006) — Dynamics of viscous vesicles in shear flow. *Eur. Phys. J. E.* **19** 389

- [7] KANTSLEER V., STEINBERG V. (2006) — Transition to tumbling and two regimes of tumbling motion of a vesicle in shear flow. *Phys. Rev. E* **96** 036001
- [8] MISBAH C. (2006) — Vacillating Breathing and Tumbling of Vesicles under Shear Flow. *Phys. Rev. Lett.* **96** 028104
- [9] OLLA P. (1997) — The lift on a tank-treading ellipsoidal cell in a shear flow. *J. Phys. II France* **7** 1533
- [10] CANTAT I., MISBAH C. (1999) — Lift Force and Dynamical Unbinding of Adhering Vesicles under Shear Flow. *Phys. Rev. Lett.* **83** 880
- [11] SUKUMARAN S., SEIFERT U. (2001) — Influence of shear flow on vesicles near a wall : a numerical study. *Phys. Rev. E* **64** 011916
- [12] ABKARIAN M., LARTIGUE C., VIALLAT A. (2002) — Tank-treading and unbinding of deformable vesicles in shear flow : determination of the lift force. *Phys. Rev. Lett.* **88** 068103
- [13] CALLENS N., MINETTI C., COUPIER G., MADER M.-A., DUBOIS F., MISBAH C., PODGORSKI T. (2008) — Hydrodynamic lift of vesicles under shear flow in microgravity. *Europhys. Lett.* **83** 24002
- [14] KAOUI B., RISTOW G., CANTAT I., MISBAH C., ZIMMERMANN W. (2008) — Lateral migration of a two-dimensional vesicle in unbounded Poiseuille flow. *Phys. Rev. E* **77** 021903
- [15] BRUINSMA R. (1996) — Rheology and shape transitions of vesicles under capillary flow. *Physica A* **234** 249
- [16] VITKOVA V., MADER M.-A., PODGORSKI T. (2004) — Deformation of vesicles flowing through capillaries. *Europhys. Lett.* **68** 398
- [17] NOGUCHI H., GOMPPER G. (2005) — Vesicle dynamics in shear and capillary flows. *J. Phys. Cond. Matter* **17** S 3439
- [18] RISSO F., COLLE-PAILLLOT F., ZAGZOULE M. (2006) — Experimental investigation of a bioartificial capsule flowing in a narrow tube. *J. Fluid. Mech.* **547** 149
- [19] SECOMB T. W., STYP-REKOWSKA B., PRIES A. R. (2007) — Two-dimensional simulation of red blood cell deformation and lateral migration in microvessels. *Ann. Biomed. Eng.* **35** 755
- [20] BAGCHI P. (2007) — Mesoscale simulation of blood flow in small vessels. *Biophys. J.* **92** 1858
- [21] MORTAZAVI S., TRYGGVASON G. (2000) — A numerical study of the motion of drops in Poiseuille flow. Part I. Lateral migration of one drop. *J. Fluid. Mech.* **411** 325
- [22] GRIGGS A. J., ZINCHENKO A. Z., DAVIS R. H. (2007) — Low-Reynolds-number motion of a deformable drop between two parallel plane walls. *Int. J. Mult. Flow* **33** 182
- [23] COUPIER G., KAOUI B., PODGORSKI T., MISBAH C. (2008) — Noninertial lateral migration of vesicles in bounded Poiseuille flow. *Phys. Fluids* **20** 111702
- [24] ANGELOVA M. I., SOLEAU S., MELEARD P., FAUCON J. F., BOTHEREL P. (1992) — Preparation of giant vesicles by external AC electric fields. Kinetics and applications. *Progr. Colloid. Polym. Sci.* **89** 127
- [25] WHITE F. M. (1991) — *Viscous Fluid Flow McGraw-Hill, New-York.*
- [26] POZRIKIDIS C. (1992) — *Boundary integral and singularity methods for linearized viscous flow Cambridge University Press.*
- [27] CANTAT I., KASSNER K., MISBAH C. (2003) — Vesicles in haptotaxis with hydrodynamical. *Eur. Phys. J. E* **10** 175
- [28] VITKOVA V., COUPIER G., MADER M.A., KAOUI B., MISBAH C., PODGORSKI T. (2009) — Tumbling of viscous vesicles in a linear shear field near a wall. *J. Optoelectron. Adv. M.*, **11** 1218.